This is a repository copy of *Positioning and contour extraction of autonomous vehicles based on enhanced DOA estimation by large-scale arrays*.

White Rose Research Online URL for this paper:
https://eprints.whiterose.ac.uk/197086/

Version: Accepted Version

Positioning and Contour Extraction of Autonomous Vehicles Based on Enhanced DOA Estimation By Large-scale Arrays

He Xu, Wei Liu, *Senior Member, IEEE*, Ming Jin, *Member, IEEE*, and Ye Tian, *Member, IEEE*

Abstract—As an important branch of internet of vehicle (IoV) systems, autonomous vehicle (AV) positioning based on direction-of-arrival (DOA) estimation has received extensive attention in recent years. In this paper, an AV positioning method under unknown mutual coupling is proposed within the framework of large-dimensional asymptotic theory (LAT). Firstly, enhanced and closed-form DOA estimation is achieved by jointly exploiting large-scale uniform linear arrays (ULAs), Toeplitz rectification and the phase transformation result associated with the sample covariance matrix; secondly, a more reliable subset/set of DOAs is constructed according to the signal-to-noise at receivers; finally, robust AV positioning is achieved with the reliable subset/set. Motivated by satisfactory DOA estimation performance, an AV contour extraction scheme is developed with the aid of two antennas installed on an AV. The proposed method shows several salient advantages compared with existing methods, including improved resolution and accuracy, reduced computational complexity, robustness to mutual coupling and unreasonable DOA estimates, as well as the ability to effectively extract AV contour information.

Index Terms—Internet of Vehicle (IoV), autonomous vehicle (AV) positioning, contour extraction, enhanced DOA estimation, large-scale ULA, mutual coupling.

I. INTRODUCTION

AS an important part of Internet of Vehicle (IoV) systems, autonomous vehicles (AVs) have become a major current innovation hotspot and development direction of the automotive industry [1]. To guarantee the safety and security of autonomous driving, the accurate location and the contour information of AVs are required. In most scenarios of IoVs, global positioning system (GPS) based vehicle positioning is a common and basic strategy [2]. However, the current commercial GPS may suffer from long latency and inadequate accuracy, which cannot meet the positioning requirements of autonomous driving in IoV business [3]. Meanwhile, for some conditions, such as tunnels and cloud cover, the GPS may fail to work. Under such circumstances, exploiting collaborative positioning methods to improve vehicle positioning accuracy,

H. Xu, M. Jin and Y. Tian are with the Faculty of Electrical Engineering and Computer Science, Ningbo University, Ningbo 315211, China (e-mail: xuhebest@sina.com; jinming@nbu.edu.cn; tianfield@126.com).

W. Liu is with the Department of Electronic and Electrical Engineering, University of Sheffield, Sheffield S1 3JD, U.K. (e-mail: w.liu@sheffield.ac.uk).

continuity and stability has become one of the key development trends in IoV systems.

Collaborative positioning techniques often estimate the positions of target vehicles with radio signal strengths (RSSs), time of arrivals (TOAs), time difference of arrivals (TDOAs) or direction of arrivals (DOAs), which are measured with reference signals at wireless communication devices, such as wireless access points (APs) and base stations (BSs) [4], [5]. In [6] and [7], RSS-based methods are proposed to achieve target vehicle positioning via multiple BSs, which have the advantage of simplicity. However, these methods require a priori knowledge of the path-loss exponents (PLEs), which is difficult to obtain accurately because of the complexity of wireless channels. In [8]–[10], TOA- and TDOA-based methods are investigated, and their performance relies on accurate synchronization of different clocks. Since perfect synchronization is not easily available among LTE BSs/nodes in practice, it is difficult for these methods to achieve a satisfactory positioning performance. Different from TOA- and TDOA-based methods, DOA-based methods are more likely to obtain accurate vehicle positioning results, because they are relatively insensitive to time delay measurements and an accurate clock synchronization is not required [11]. As a competitive candidate, several DOA positioning methods utilizing LTE BSs or wireless APs have been investigated [12]. Recently, by combining DOA and TOA or DOA and TDOA, the matrix pencil (MP) method and the semi-definite programming (SDP) method for positioning using LTE signals are introduced in [13] and [14], respectively. However, like TOA- and TDOA-based methods, these joint methods are also sensitive to delay measurements. With this consideration, in this work, we focus on a DOA-based AV positioning architecture.

Many DOA estimation methods have been developed under different frameworks, such as the traditional multiple signal classification (MUSIC) method [15], the estimation of signal parameters via rotational invariance techniques (ESPRIT) [16] and their variations [17]–[22] in the classical asymptotic theory (CAT) framework; the G-MUSIC method [23], the conditional G-MUSIC method [24] and the R-MUSIC method [25] in the large-dimensional asymptotic theory (LAT) framework; the matching pursuit based methods [26], [27], the ℓ_1-norm minimization based methods [28]–[30], and the sparse Bayesian learning (SBL) based methods in the sparse representation (SR) framework [31], [32]. In particular, the MUSIC-like [33] and the SBL [34] based methods are proposed for vehicle

positioning in IoV systems in the past few years, and these two are good attempts for vehicle localization from a DOA estimation perspective. However, they still face the following challenges when applied to vehicle positioning in an actual IoV environment.

- The existing DOA-based vehicle positioning methods are normally developed for small-scale arrays and exploit spectral search to achieve DOA estimation. As a result, they suffer from not only performance degeneration in closely-spaced vehicle scenarios due to insufficient array aperture, but also high computational complexity, which makes them difficult to meet the actual needs of autonomous driving in terms of positioning accuracy and complexity.
- Most of existing DOA estimators are based on ideal/well-calibrated sensor arrays. However, in practice, array uncertainties, such as the mutual coupling, gain-phase errors and sensor location errors always exist, which could degrade the DOA estimation performance substantially [35]–[37]. Although the MUSIC-like method in [33] takes the unknown mutual coupling into consideration, the spectral search cannot be avoided.
- Both the MUSIC-like method [33] and the SBL method [34] utilize multiple DOAs provided by the BSs or wireless APs directly for vehicle localization. In fact, due to the influence of factors such as the transmission loss and the incident angle, not all DOA estimates are accurate enough and how to choose the best subset of estimation results in order to achieve a robust performance is still a challenge.

To tackle the mentioned problems above, an AV positioning and contour extraction method is proposed in this work, employing large-scale uniform linear arrays (ULAs) with unknown mutual coupling. Different from the existing DOA-based vehicle localization methods, the proposed one is developed in the LAT framework, leading to an improved AV positioning performance. The main contributions of the work are:

1) Instead of utilizing general small-scale arrays, large-scale ULAs are employed, and the impact of unknown mutual coupling and finite samples for the high-dimensional scenario is considered. In the proposed approach, firstly, a linear transformation is performed for eliminating unknown mutual coupling; then, a two-stage strategy which jointly exploit the Toeplitz rectification and the phase transformation in the LAT framework is developed for improving the estimation of sample covariance matrix (SCM) and its corresponding eigenvectors, leading to a super-resolution and closed-form DOA estimate. To our best knowledge, it is the first time to apply this two-stage statistical enhancement to achieving vehicle localization in the field of IoV. Moreover, it should be emphasized here that the considered scenario matches well with the application scenarios of AVs in 5G/6G IoV systems, representing a good step in the realization of highly reliable autonomous driving of AVs.

2) Instead of using DOA estimates provided by multiple base stations (BSs) directly, we exploit information about the received SNR and the relationship between estimation accuracy and incident angle to select a reliable subset/set of DOA estimates, and then achieve robust vehicle positioning with those preferred DOA information. As demonstrated by simulations, it is a simple but very effective method and it is also the first time to apply such a method to promoting the robustness of DOA-based vehicle positioning.

3) The proposed positioning method can yield decimeter or even centimeter-level positioning accuracy even for closely-spaced vehicle scenarios. When SNR ≥ 10 dB, and the numbers of sensors and samples are 80 and 100, respectively, the proposed method can yield a positioning accuracy within 0.3 m with 100% availability, and be carried out in less than nine milliseconds on MATLAB with a 2.0 GHz CPU. That is, the method can meet the requirements of absolute position accuracy, service availability and latency in 5G standardization in conformance with the 3rd Generation Partnership Project (3GPP) TS 22.261 [38], [39].

4) Due to the high positioning accuracy, we further extract contour information of the vehicle with the aid of two antennas installed. In detail, a configuration scheme for antennas is first designed, and then information about vehicle moving direction and the location of two antennas is exploited to achieve coarse contour estimation of the vehicle. Moreover, the fundamental requirement for the two antennas on DOA separation for contour extraction is analyzed and the feasibility of this scheme is validated by numerical simulations. In literature, contour extraction of vehicles is almost always achieved by various imaging methods. To our best knowledge, this is the first time to approach this problem from the DOA-based perspective, which provides another simple but effective tool for tackling this challenge.

The remainder of this article is organized as follows. In Section II, an AV positioning system using three collaborative BSs, and the data model for DOA estimation with large-scale ULAs with unknown mutual coupling are presented. The enhanced DOA estimation method is described in Section III. The robust AV positioning and contour extraction scheme is demonstrated in Section IV. Numerical examples are provided in Section V, and conclusions are drawn in Section VI.

Notations: Capital boldface letters, lower-case boldface letters and lower-case italic letters are used to represent matrices, vectors and scalars, respectively. Superscripts $(\cdot)^*, (\cdot)^T, (\cdot)^H$ and $(\cdot)^{-1}$ and $(\cdot)^\dagger$ represent the conjugate, transpose, conjugate transpose, inverse and pseudo inverse operators, respectively. $\mathbb{E}\{\cdot\}$ stands for the statistical expectation, $\odot$, diag$\{\cdot\}$ and det$[\cdot]$ denote the Hadamard Schur product, diagonalization and determinant operators, respectively. Moreover, $\mathbf{I}_M$ is the $M \times M$ identity matrix, $\mathbf{J}^m$ is the $M \times M$ shift matrix, whose elements on the mth superdiagonal equal 1 and 0 elsewhere, and $\mathbf{0}_{M \times N}$ is the $M \times N$-dimensional all-zero matrix. $\angle[\cdot]$ represents the phase of a complex number, and Teoplitz$\{\mathbf{r}\}$
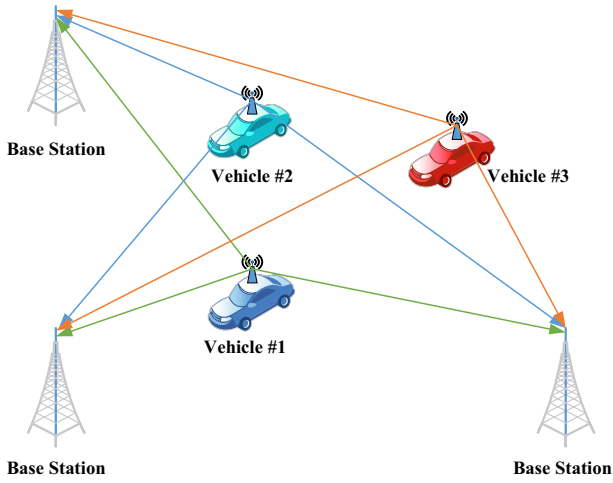
Fig. 1. Illustration of AV positioning system using multiple BSs.

the symmetric Toeplitz matrix constructed by the vector $\mathbf{r}$. $\mathrm{Re}\{\cdot\}$ and $\mathrm{Im}\{\cdot\}$ stand for the real part and imaginary part of a complex value, respectively. $\mathrm{tr}\{\cdot\}$ represents the trace of a matrix. Finally, $\|\cdot\|$, $\mathcal{N}(\cdot)$, $\xrightarrow{a.s.}$ and $\xrightarrow{D}$ indicate the spectral norm, the normal distribution, almost certain convergence and convergence in distribution, respectively.

II. POSITIONING SYSTEM AND DATA MODEL

Consider an AV positioning system shown in Fig. 1, where three collaborative BSs are employed, each equipped with a large M-element ULA with interspacing d. By assumption, all the three BSs are configured to work in the same way. Each AV terminal carries a wireless signal transmitter with a unique identification label. The BS first estimates the DOA of the target vehicle, and then applies the cross-positioning principle to achieve AV localization. The key point lies in a robust and accurate DOA estimation. For simplicity, it is assumed that there are K AVs on the same plane, whose transmitted signals are uncorrelated and impinge on a BS from distinct DOAs θ_k, $k = 1, \ldots, K$. Using the first element of the ULA as the phase reference point, the received array signal at a BS at time instant t can be expressed as

$$\mathbf{y}(t) = \mathbf{CAs}(t) + \mathbf{n}(t) = \sum_{k=1}^{K} \mathbf{a}(\theta_k) s_k(t) + \mathbf{n}(t) \quad (1)$$

where $\mathbf{y}(t) = [y_1(t), \ldots, y_M(t)]^T \in \mathbb{C}^{M \times 1}$, $\mathbf{s}(t) = [s_1(t), \ldots, s_K(t)]^T \in \mathbb{C}^{K \times 1}$, $\mathbf{n}(t) = [n_1(t), \ldots, n_M(t)]^T \in \mathbb{C}^{M \times 1}$, $\mathbf{A} = [\mathbf{a}(\theta_1), \ldots \mathbf{a}(\theta_k), \ldots, \mathbf{a}(\theta_K)]^T \in \mathbb{C}^{M \times K}$, $\mathbf{a}(\theta_k) = [1, e^{-jw_k}, \ldots, e^{-j(M-1)w_k}]^T \in \mathbb{C}^{M \times 1}$ and $w_k = 2\pi d \sin \theta_k / \lambda$ with λ denoting the carrier wavelength. $\mathbf{C} \in \mathbb{C}^{M \times M}$ is a mutual coupling matrix (MCM) with a symmetric Toeplitz structure. In practice, the mutual coupling coefficients are approximately zero when the distance between antennas is larger than a given threshold; thus, $\mathbf{C}$ is typically expressed as

$$\mathbf{C} = \mathrm{Toeplitz}\{[1, c_1, \ldots, c_P, 0, \ldots, 0]\} \quad (2)$$

where $0 < |c_P| < \cdots < |c_1| < 1$ and $P < M$.

Suppose that the noise $\mathbf{n}(t)$ is zero-mean, complex white Gaussian distributed and is independent of the signal $\mathbf{s}(t)$, the covariance matrix of $\mathbf{y}(t)$ is given by

$$\mathbf{R}_y = \mathbb{E}\{\mathbf{y}(t)\mathbf{y}^H(t)\} = \mathbf{CAP}_s\mathbf{A}^H\mathbf{C}^H + \sigma_n^2\mathbf{I}_M \in \mathbb{C}^{M \times M} \quad (3)$$

where $\mathbf{P}_s = \mathrm{diag}\{\sigma_1^2, \sigma_2^2, \ldots, \sigma_K^2\}$ with σ_k^2 representing the received signal power of the kth source, and σ_n^2 is the variance of additive noise. In case of N samples, $\mathbf{R}_y$ can be estimated by the unstructured SCM

$$\hat{\mathbf{R}}_y = \frac{1}{N} \sum_{t=1}^{N} \mathbf{y}(t)\mathbf{y}^H(t) \in \mathbb{C}^{M \times M}. \quad (4)$$

For the classical asymptotic case where M is fixed and $N \to \infty$, $\hat{\mathbf{R}}_y$ is a consistent estimator of $\mathbf{R}_y$. Unfortunately, in actual IoV scenarios for AV positioning utilizing large-scale arrays, the number of available samples N is limited and normally of the same order as the number of sensors M, since the location of the fast-moving AVs can only be assumed to be fixed for a very short period of time. In this situation, $\hat{\mathbf{R}}_y$ is no longer a good estimator of $\mathbf{R}_y$ [40]. In the following, we will develop an efficient scheme to achieve satisfactory DOA and positioning results in the scenario where N is of the same order as M, to meet the requirement of an actual AV positioning.

III. ENHANCED DOA ESTIMATION

A. Mutual Coupling Elimination

The symmetric Toeplitz structure of MCM can be exploited to eliminate its influence. Defining $\mathbf{T} = [\mathbf{0}_{(M-2P) \times P}, \mathbf{I}_{M-2P}, \mathbf{0}_{(M-2P) \times P}]$, we have

$$\breve{\mathbf{R}}_y = \mathbf{T}\mathbf{R}_y\mathbf{T}^T = \breve{\mathbf{A}}\bar{\mathbf{C}}\mathbf{P}_s\bar{\mathbf{C}}^H\breve{\mathbf{A}}^H + \sigma_n^2\mathbf{I}_{M-2P}, \quad (5)$$

where $\breve{\mathbf{A}} = [\breve{\mathbf{a}}(\theta_1), \ldots, \breve{\mathbf{a}}(\theta_K)]$ consists of the middle $\bar{M} = M - 2P$ rows of $\mathbf{A}$, and $\bar{\mathbf{C}} = \mathrm{diag}\{\bar{\sigma}_1^2, \bar{\sigma}_2^2, \ldots, \bar{\sigma}_K^2\}$ with $\bar{\sigma}_k^2 = \sum_{p=-P}^{P} c_{|p|} e^{-jpw_k}$.

It is interesting to see that the mutual coupling coefficients are embedded in the diagonal matrix $\bar{\mathbf{C}}$, which implies that the influence of unknown mutual coupling is eliminated effectively. On the other hand, it can be further observed that the SCM is transformed from the Hermitian structure into a complex Toeplitz structure, which in fact provides a basic condition for the enhancement of SCM in the next subsection.

Remark 1: It can be observed from (5) that the application of linear transformation has reduced the array aperture by $2P$, which is a drawback and reduces the maximum number of resolvable sources. However, since for most practical scenarios we usually have $P = 2$ or 3 [41], [42], given the large-scale array employed for IoV applications ($M \gg P$), such an array aperture loss will have a minimal/tolerable effect.

B. Two-stage Strategy for Enhanced DOA Estimation

To obtain a robust and optimal DOA estimate, a two-stage statistical enhancement method is adopted. The first stage is to enhance the SCM via Toeplitz rectification, while the second

stage is to enhance eigenvalues and eigenvectors by exploiting the asymptotic property of the "spiked" covariance matrix.

Stage A: Toeplitz rectification is a widely used approach to improve the SCM that holds a Toeplitz structure statistically [43]. For an $\bar{M} \times \bar{M}$ matrix $\boldsymbol{\Upsilon}$, the process of Toeplitz rectification is performed as

$$\Xi\left(\boldsymbol{\Upsilon}\right) = \sum_{m=-\bar{M}+1}^{\bar{M}-1} \frac{1}{\bar{M}-|m|} \mathrm{Tr}\left(\boldsymbol{\Upsilon}\mathbf{J}^m\right)\mathbf{J}^{-m}, \quad (6)$$

where $\mathbf{J}^{-m}$ stands for $(\mathbf{J}^m)^T$, and $\mathbf{J}^0 = \mathbf{I}_{\bar{M}}$. Subsequently, the rectified SCM can be given by

$$\breve{\mathbf{R}}_r = \Xi(\widehat{\mathbf{R}}_y), \quad (7)$$

where $\widehat{\mathbf{R}}_y$ stands for the estimation of $\breve{\mathbf{R}}_y$ with N samples. The rectified SCM $\hat{\mathbf{R}}_r$ leads to a norm-consistent estimator, which implies that the converge $||\breve{\mathbf{R}}_r - \breve{\mathbf{R}}_y|| \xrightarrow{a.s.} 0$ holds as $\bar{M}, N \to \infty$, and $\bar{M}/N = c \in (0, \infty)$ [25].

Suppose that the number of sources K is estimated accurately with the linear shrinkage based minimum description length (LS-MDL) [44] or the bayesian information criterion (BIC) variant [45] criterion, then, by performing eigenvalue decomposition (EVD) on $\breve{\mathbf{R}}_r$, we have

$$\breve{\mathbf{R}}_r = \hat{\mathbf{U}}_s \hat{\boldsymbol{\Sigma}}_s \hat{\mathbf{U}}_s^H + \hat{\mathbf{U}}_n \hat{\boldsymbol{\Sigma}}_n \hat{\mathbf{U}}_n^H, \quad (8)$$

where $\hat{\boldsymbol{\Sigma}}_s = \mathrm{diag}\{\hat{\lambda}_1, \ldots, \hat{\lambda}_K\}$, $\hat{\boldsymbol{\Sigma}}_n = \mathrm{diag}\{\hat{\lambda}_{K+1}, \ldots, \hat{\lambda}_M\}$, and $\hat{\lambda}_i(i = 1, \ldots, M)$ are eigenvalues of $\hat{\mathbf{R}}_r$ in descending order. $\hat{\mathbf{U}}_s \in \mathbb{C}^{M \times K}$ and $\hat{\mathbf{U}}_n \in \mathbb{C}^{M \times (M-K)}$ are the signal subspace and the noise subspace corresponding to $\hat{\boldsymbol{\Sigma}}_s$ and $\hat{\boldsymbol{\Sigma}}_n$, respectively. According to the subspace theory, the following relationship holds

$$\begin{bmatrix} \hat{\mathbf{U}}_{s1} \\ \hat{\mathbf{U}}_{s2} \end{bmatrix} = \begin{bmatrix} \breve{\mathbf{A}}_1 \bar{\mathbf{C}} \\ \breve{\mathbf{A}}_2 \bar{\mathbf{C}} \end{bmatrix} \mathbf{G} = \begin{bmatrix} \breve{\mathbf{A}}_1 \\ \breve{\mathbf{A}}_1 \boldsymbol{\Psi} \end{bmatrix} \bar{\mathbf{G}}, \quad (9)$$

where $\hat{\mathbf{U}}_{s1}$ ($\hat{\mathbf{U}}_{s2}$) and $\breve{\mathbf{A}}_1$ ($\breve{\mathbf{A}}_2$) are the first (last) $\bar{M}-1$ rows of $\hat{\mathbf{U}}_s$ and $\breve{\mathbf{A}}$, respectively. $\boldsymbol{\Psi} = \mathrm{diag}\{e^{-jw_1}, \ldots, e^{-jw_K}\}$, $\mathbf{G} \in \mathbb{C}^{K \times K}$ and $\bar{\mathbf{G}} = \bar{\mathbf{C}}\mathbf{G} \in \mathbb{C}^{K \times K}$ are matrices.

Defining $\boldsymbol{\Gamma} = \bar{\mathbf{G}}^{-1}\boldsymbol{\Psi}\bar{\mathbf{G}}$, the estimate of $\boldsymbol{\Gamma}$ is given by

$$\hat{\boldsymbol{\Gamma}} = \hat{\mathbf{U}}_{s1}^{\dagger}\hat{\mathbf{U}}_{s2}. \quad (10)$$

It is clear that the eigenvalues of $\hat{\boldsymbol{\Gamma}}$ is just the estimates of the diagonal elements of $\boldsymbol{\Psi}$, which means that the DOAs of K sources can be estimated as

$$\hat{\theta}_k = \sin^{-1}\left(-\lambda\angle[\gamma_k]/2\pi d\right), k = 1, \ldots, K, \quad (11)$$

where γ_k is the kth eigenvalue of $\hat{\boldsymbol{\Gamma}}$.

It has been studied that Toeplitz rectification can yield an improved DOA estimation performance, provided that SNR is not sufficiently high [25]. Unfortunately, in high SNR situations, their corresponding estimators often suffer from the so-called "saturation phenomenon" (see the corresponding simulation results in [25] for details), primarily because the difference $|| \sum_{t=1}^{N} \mathbf{s}(t)\mathbf{s}^H(t)/N - \mathbf{P}_s ||$ converges to 0 at a rate slower than $O(N^{-1/2})$. As a result, the unbiased signal subspace cannot be achieved regardless of SNR.

Stage B: To tackle the problem associated with the "saturation phenomenon", the asymptotic properties of eigenvalues and eigenvectors of $\breve{\mathbf{R}}_r$ are exploited. Note that $\breve{\mathbf{R}}_r$ can be regarded as a kind of "spiked" covariance matrix [46], whose convergence characteristics of K largest eigenvalues $\hat{\lambda}_1, \ldots, \hat{\lambda}_K$ and their corresponding eigenvectors $\hat{\mathbf{u}}_1, \ldots, \hat{\mathbf{u}}_K$ under the case that $\bar{M}, N \to \infty$, and $\bar{M}/N = c \in (0, \infty)$ satisfy

$$\hat{\lambda}_k \xrightarrow{a.s.} \begin{cases} \frac{(\sigma_n^2 + \alpha_k)(\sigma_n^2 c + \alpha_k)}{\alpha_k}, & \alpha_k > \sigma_n^2\sqrt{c} \\ \sigma_n^2(1 + \sqrt{c})^2, & \alpha_k \le \sigma_n^2\sqrt{c}, \end{cases} \quad (12)$$

$$|\hat{\mathbf{u}}_k^H \mathbf{w}_k|^2 \xrightarrow{a.s.} \begin{cases} \frac{\alpha_k^2 - \sigma_n^4 c}{\alpha_k(\alpha_k + \sigma_n^2 c)}, & \alpha_k \ge \sigma_n^2\sqrt{c} \\ 0, & \alpha_k \le \sigma_n^2\sqrt{c}, \end{cases} \quad (13)$$

where α_k and $\mathbf{w}_k$ stand for the true eigenvalues and eigenvectors of $\breve{\mathbf{A}}\bar{\mathbf{C}}\mathbf{P}_s\bar{\mathbf{C}}^H\breve{\mathbf{A}}^H$, respectively.

According to (12) and (13), we can further derive that the following holds

$$\tilde{\alpha}_k = \frac{1}{2}\{\hat{\lambda}_k - \hat{\sigma}_n^2(1+c) + \sqrt{[\hat{\lambda}_k - \hat{\sigma}_n^2(1+c)]^2 - 4\hat{\sigma}_n^2 c}\}, \quad (14)$$

$$\sqrt{\bar{M}}(\hat{\mathbf{u}}_k - \beta_k \mathbf{w}_k) \xrightarrow{D} \mathcal{N}(\mathbf{0}, (1 - \beta_k^2)\mathbf{I}_{\bar{M}}), \quad (15)$$

where $\hat{\sigma}_n^2 = \frac{1}{\bar{M}-K}\sum_{i=K+1}^{\bar{M}} \hat{\lambda}_i$, $\beta_k = \frac{\tilde{\alpha}_k^2 - \hat{\sigma}_n^4 c}{\tilde{\alpha}_k(\tilde{\alpha}_k + \hat{\sigma}_n^2 c)}$. Formulation (15) implies that $\hat{\mathbf{u}}_k$ can be written as

$$\hat{\mathbf{u}}_k = \beta_k \mathbf{w}_k + \bar{\mathbf{n}}_k, k = 1, \ldots, K, \quad (16)$$

where $\bar{\mathbf{n}}_k \in \mathbb{C}^{\bar{M} \times 1}$ is a random vector with $\mathbb{E}\{\bar{\mathbf{n}}_k\} = \mathbf{0}$ and $\mathbb{E}\{\bar{\mathbf{n}}_k \bar{\mathbf{n}}_k^H\} = \sqrt{\frac{1-\beta_k^2}{\bar{M}}}\mathbf{I}_{\bar{M}}$.

Motivated by the fact that $\sqrt{(1 - \varphi_k^2)/\bar{M}} \to 0$ as $\bar{M} \to \infty$, $\bar{\mathbf{n}}_k$ is omitted here, and subsequently we have

$$\hat{\mathbf{u}}_k \approx \beta_k \mathbf{w}_k, k = 1, \ldots, K. \quad (17)$$

With (17), the enhanced signal subspace is constructed as

$$\mathbf{U}_s = [\bar{\beta}_1^{-1}\hat{\mathbf{u}}_1, \ldots, \bar{\beta}_K^{-1}\hat{\mathbf{u}}_K]. \quad (18)$$

Finally, DOA estimation is performed after replacing $\hat{\mathbf{U}}_s$ with $\mathbf{U}_s$. Let $\hat{\theta}_k$ denote the estimated DOA of the kth source and $\mathbf{c} = [1, c_1, \ldots, c_P]^T$. Since $\bar{\mathbf{a}}(\theta_k)\bar{\sigma}_k^2 = \mathbf{B}(\theta_k)\mathbf{c}$ and $\mathbf{E}_n^H \bar{\mathbf{a}}(\theta_k)\bar{\sigma}_k^2 = \mathbf{0}_{(\bar{M}-K)\times 1}$, we have

$$\mathbf{E}_n^H \mathbf{B}(\theta_k)\mathbf{c} = \mathbf{0}_{(\bar{M}-K)\times 1}, \quad (19)$$

$$\mathbf{B}(\theta_k) = \begin{bmatrix} e^{-jPw_k} & e^{-j(P-1)w_k} + e^{-j(P+1)w_k} & \cdots & 1 + e^{-j2Pw_k} \\ e^{-j(P+1)w_k} & e^{-jPw_k} + e^{-j(P+2)w_k} & \cdots & e^{-jPw_k} + e^{-j(2P+1)w_k} \\ \vdots & \vdots & \cdots & \vdots \\ e^{-j(M-P-1)w_k} & e^{-j(M-P-2)w_k} + e^{-j(M-P)w_k} & \cdots & e^{-j(M-2P-1)w_k} + e^{-j(M-1)w_k} \end{bmatrix}.$$

Algorithm 1: Two-stage Strategy for DOA Estimation

1: Calculate the SCM $\hat{\mathbf{R}}_y$ with N samples, and carry out linear transformation using $\mathbf{T}$ to get $\widehat{\mathbf{R}}_y$.

Stage A:

2: Form the rectified SCM $\breve{\mathbf{R}}_r$ via Toeplitz rectification.

3: Perform EVD on $\breve{\mathbf{R}}_r$ to obtain $\hat{\lambda}_k$ and $\hat{\mathbf{u}}_k$, $k \in [1, K]$.

Stage B:

4: Calculate $\tilde{\alpha}_k$ and $\hat{\mathbf{u}}_k$ by (14) and (17), respectively.

5: Construct the enhanced signal subspace $\mathbf{U}_s$ according to (18), and further divide it into $\hat{\mathbf{U}}_{s1}$ and $\hat{\mathbf{U}}_{s2}$.

6: Obtain the estimate of $\mathbf{\Gamma}$ by $\hat{\mathbf{\Gamma}} = \hat{\mathbf{U}}_{s1}^{\dagger}\hat{\mathbf{U}}_{s2}$.

7: Perform EVD on $\hat{\mathbf{\Gamma}}$ to obtain eigenvalues $\gamma_1, \ldots, \gamma_K$.

8: Estimate K DOAs by $\hat{\theta}_k = \sin^{-1}(-\lambda\angle[\gamma_k]/2\pi d)$.

9: Form $\mathbf{Q}_k$ and further estimate $\mathbf{c}$ based on (21).

---

where $\mathbf{E}_n \in \mathbb{C}^{\bar{M}\times(\bar{M}-K)}$ denotes the noise subspace of $\bar{\mathbf{R}}_x$, and $\mathbf{B}(\theta_k) \in \mathbb{C}^{\bar{M}\times(P+1)}$ is given at the bottom of this page.

Define $\mathbf{Q}_k = \mathbf{B}^H(\theta_k)\mathbf{E}_n\mathbf{E}_n^H\mathbf{B}(\theta_k)$, and then the mutual coupling estimation problem can be transformed into the following optimization problem,

$$\min \ \mathbf{c}^H\mathbf{Q}_k\mathbf{c}, \ s.\,t. \ \mathbf{d}^T\mathbf{c} = 1, \tag{20}$$

where $\mathbf{d} = [1, 0, \ldots, 0]^T$. By using the well-known Lagrange multiplier method, $\mathbf{c}$ can be estimated by

$$\hat{\mathbf{c}} = \frac{1}{K}\sum_{k=1}^{K}\frac{\mathbf{Q}_k^{-1}\mathbf{d}}{\mathbf{d}^T\mathbf{Q}_k^{-1}\mathbf{d}}. \tag{21}$$

The proposed two-stage strategy for enhanced DOA estimation is summarized in **Algorithm 1**.

Remark 2: The proposed method is computationally more efficient than the MUSIC-Like method [33]. For the latter, the major computations involved are to form one $M \times M$ SCM, to perform its EVD and to conduct a spectrum search, whose total number of complex multiplications required is $\mathcal{O}\{M^2N + \frac{4}{3}M^3 + M^2(P+1)G + M(P+1)^2G\}$, where G is the number of searching grids. For the proposed method, the major computations involved are only to form one $\bar{M} \times \bar{M}$ SCM and to perform its EVD, and the process of mutual coupling estimation can be avoided since it is not necessary for DOA estimation. Therefore, the total number of multiplications required is $\mathcal{O}\{\bar{M}^2N + \frac{4}{3}\bar{M}^3\}$, which is much lower than the MUSIC-Like method.

C. Cramér-Rao Bound

The Cramér-Rao Bound (CRB) serves as the benchmark for the performance analysis, which is obtained by taking the inverse of the Fisher information matrix (FIM). The vector of unknown parameters is given by

$$\boldsymbol{\eta} = \left[\boldsymbol{\theta}^T, \boldsymbol{\kappa}^T, \boldsymbol{\xi}^T\right]^T \tag{22}$$

where $\boldsymbol{\theta} = [\theta_1, \ldots, \theta_K]$, $\boldsymbol{\kappa} = \mathrm{Re}\{\mathbf{c}\}$ and $\boldsymbol{\xi} = \mathrm{Im}\{\mathbf{c}\}$. Then, the (m, n)th element of the FIM is given by

$$\mathbf{F}_{m,n} = N\mathrm{tr}\left\{\mathbf{R}_y^{-1}\frac{\partial \mathbf{R}_y}{\partial \eta_m}\mathbf{R}_y^{-1}\frac{\partial \mathbf{R}_y}{\partial \eta_n}\right\}. \tag{23}$$

Defining $\dot{\mathbf{A}} = [\partial\mathbf{a}(\theta_1)/\partial\theta_1, \ldots, \partial\mathbf{a}(\theta_K)/\partial\theta_K]$, $\bar{\mathbf{A}} = \mathbf{C}\mathbf{A}$, $\dot{\mathbf{C}}_{\kappa_m} = -j \cdot \dot{\mathbf{C}}_{\xi_m} = \mathrm{Toeplitz}\left[0, \mathbf{e}_m^T, \mathbf{0}_{1\times(M-P-1)}\right]$, where $\mathbf{e}_m$ is the P-dimensional column vector with 1 at its m-th element and 0 elsewhere, we can obtain that [47], [48]

$$\mathbf{F}_{\theta\theta} = 2N\mathrm{Re}\Big\{(\mathbf{P}_s\bar{\mathbf{A}}^H\mathbf{R}_y^{-1}\bar{\mathbf{A}}\mathbf{P}_s)\odot(\dot{\mathbf{A}}^H\mathbf{C}^H\mathbf{R}_y^{-1}\mathbf{C}\dot{\mathbf{A}})^T$$
$$+ (\mathbf{P}_s\bar{\mathbf{A}}^H\mathbf{R}_y^{-1}\mathbf{C}\dot{\mathbf{A}})\odot(\mathbf{P}_s\bar{\mathbf{A}}^H\mathbf{R}_y^{-1}\mathbf{C}\dot{\mathbf{A}})^T\Big\}$$

$$\mathbf{F}_{\theta\kappa_n} = 2N\mathrm{Re}\Big\{\mathrm{diag}\left\{\mathbf{P}_s\bar{\mathbf{A}}^H\mathbf{R}_y^{-1}\dot{\mathbf{C}}_{\kappa_n}\mathbf{A}\mathbf{P}_s\bar{\mathbf{A}}^H\mathbf{R}_y^{-1}\mathbf{C}\dot{\mathbf{A}}\right\}$$
$$+ \mathrm{diag}\left\{\mathbf{P}_s\bar{\mathbf{A}}^H\mathbf{R}_y^{-1}\bar{\mathbf{A}}\mathbf{P}_s\mathbf{A}^H\dot{\mathbf{C}}_{\kappa_n}\mathbf{R}_y^{-1}\mathbf{C}\dot{\mathbf{A}}\right\}\Big\}$$

$$\mathbf{F}_{\theta\xi_n} = 2N\mathrm{Re}\Big\{\mathrm{diag}\left\{\mathbf{P}_s\bar{\mathbf{A}}^H\mathbf{R}_y^{-1}\dot{\mathbf{C}}_{\xi_n}\mathbf{A}\mathbf{P}_s\bar{\mathbf{A}}^H\mathbf{R}_y^{-1}\mathbf{C}\dot{\mathbf{A}}\right\}$$
$$+ \mathrm{diag}\left\{\mathbf{P}_s\bar{\mathbf{A}}^H\mathbf{R}_y^{-1}\bar{\mathbf{A}}\mathbf{P}_s\mathbf{A}^H\dot{\mathbf{C}}_{\xi_n}\mathbf{R}_y^{-1}\mathbf{C}\dot{\mathbf{A}}\right\}\Big\}$$

$$\mathbf{F}_{\kappa_m\kappa_n} = 2N\mathrm{Re}\Big\{\mathrm{tr}\left\{\mathbf{R}_y^{-1}\dot{\mathbf{C}}_{\kappa_m}\mathbf{A}\mathbf{P}_s\bar{\mathbf{A}}^H\mathbf{R}_y^{-1}\bar{\mathbf{A}}\mathbf{P}_s\mathbf{A}^H\dot{\mathbf{C}}_{\kappa_n}\right\}$$
$$+ \mathrm{tr}\left\{\mathbf{R}_y^{-1}\dot{\mathbf{C}}_{\kappa_m}\mathbf{A}\mathbf{P}_s\bar{\mathbf{A}}^H\mathbf{R}_y^{-1}\dot{\mathbf{C}}_{\kappa_n}\mathbf{A}\mathbf{P}_s\bar{\mathbf{A}}^H\right\}\Big\}$$

$$\mathbf{F}_{\kappa_m\xi_n} = 2N\mathrm{Re}\Big\{\mathrm{tr}\left\{\mathbf{R}_y^{-1}\dot{\mathbf{C}}_{\kappa_m}\mathbf{A}\mathbf{P}_s\bar{\mathbf{A}}^H\mathbf{R}_y^{-1}\bar{\mathbf{A}}\mathbf{P}_s\mathbf{A}^H\dot{\mathbf{C}}_{\xi_n}\right\}$$
$$+ \mathrm{tr}\left\{\mathbf{R}_y^{-1}\dot{\mathbf{C}}_{\kappa_m}\mathbf{A}\mathbf{P}_s\bar{\mathbf{A}}^H\mathbf{R}_y^{-1}\dot{\mathbf{C}}_{\xi_n}\mathbf{A}\mathbf{P}_s\bar{\mathbf{A}}^H\right\}\Big\}$$

$$\mathbf{F}_{\xi_m\xi_n} = 2N\mathrm{Re}\Big\{\mathrm{tr}\left\{\mathbf{R}_y^{-1}\dot{\mathbf{C}}_{\xi_m}\mathbf{A}\mathbf{P}_s\bar{\mathbf{A}}^H\mathbf{R}_y^{-1}\bar{\mathbf{A}}\mathbf{P}_s\mathbf{A}^H\dot{\mathbf{C}}_{\xi_n}\right\}$$
$$+ \mathrm{tr}\left\{\mathbf{R}_y^{-1}\dot{\mathbf{C}}_{\xi_m}\mathbf{A}\mathbf{P}_s\bar{\mathbf{A}}^H\mathbf{R}_y^{-1}\dot{\mathbf{C}}_{\xi_n}\mathbf{A}\mathbf{P}_s\bar{\mathbf{A}}^H\right\}\Big\}.$$

Consequently, $\mathbf{F}$ is given by

$$\mathbf{F} = \begin{pmatrix} \mathbf{F}_{\theta\theta} & \mathbf{F}_{\theta\kappa} & \mathbf{F}_{\theta\xi} \\ \mathbf{F}_{\kappa\theta} & \mathbf{F}_{\kappa\kappa} & \mathbf{F}_{\kappa\xi} \\ \mathbf{F}_{\xi\theta} & \mathbf{F}_{\xi\kappa} & \mathbf{F}_{\xi\xi} \end{pmatrix}. \tag{24}$$

Finally, the CRB for DOA estimation can be obtained by taking the inverse of $\mathbf{F}$ as

$$\mathrm{CRB}_\theta = \sqrt{\frac{1}{K}\sum_{i=1}^{K}[\mathbf{F}^{-1}]_{ii}}. \tag{25}$$

IV. VEHICLE POSITIONING AND CONTOUR EXTRACTION

A. Vehicle Positioning

For simplicity, three collaborative BSs with known coordinates $B_1(L_{1x}, L_{1y})$, $B_2(L_{2x}, L_{2y})$, and $B_3(L_{3x}, L_{3y})$ are employed for the AV localization, as illustrated in Fig. 1. Consider an AV with its center point located at $S(x, y)$ and its DOAs corresponding to three BSs are θ_{k1}, θ_{k2}, and θ_{k3}, respectively. Then, the following equations hold,

$$\tan\theta_{k1} = \frac{L_{1y} - y}{x - L_{1x}}, \tag{26}$$

$$\tan\theta_{k2} = \frac{y - L_{2y}}{x - L_{2x}}, \tag{27}$$

$$\tan\theta_{k3} = \frac{L_{3x} - x}{y - L_{3y}}, \tag{28}$$

and $S(x, y)$ can be determined by

$$\begin{cases} x_1 = \frac{L_{1y} - L_{2y} + L_{1x}\tan\theta_{k1} + L_{2x}\tan\theta_{k2}}{\tan\theta_{k1} + \tan\theta_{k2}} \\ y_1 = \frac{L_{1y}\tan\theta_{k2} + L_{2y}\tan\theta_{k1} + (L_{1x} - L_{2x})\tan\theta_{k1}\tan\theta_{k2}}{\tan\theta_{k1} + \tan\theta_{k2}} \end{cases} \tag{29}$$

Algorithm 2: Procedure to Select Reliable Subset/Set of DOAs

Input: The rectified $\breve{\mathbf{R}}_r$, DOAs $\{\theta_{k1}, \theta_{k2}, \theta_{k3}\}$ given by three BSs, and received SNRs. The number of reliable DOAs τ, with its initialization $\tau = 3$. $\epsilon_1 = 2$ dB, $\epsilon_2 = 75°$.

Output: Reliable subset/set of DOAs and the AV location.

1: **if** $\max(\text{SNR}_{i,k}) - \min(\text{SNR}_{i,k}) > \epsilon_1$
    Remove the DOA $\theta_{k\bar{i}}$ corresponding to $\min(\text{SNR}_{i,k})$, $\tau \leftarrow \tau - 1$.

2: **else if** $\max(|\theta_{ki}|) > \epsilon_2$
    Remove the DOA $\theta_{k\bar{i}}$ corresponding to $\max(|\theta_{ki}|)$, $\tau \leftarrow \tau - 1$.

3: **end**

4: **if** $\tau = 2$
    Output reliable subset of DOAs, consisting of the remaining two DOAs, and determine the AV location by (29) or (30) or (31).

5: **else**
    Output reliable set of DOAs, consisting of all the three DOAs, and determine the AV location by (32).

6: **end**

---

or

$$\begin{cases} x_2 = \frac{(L_{1y} - L_{3y})\tan\theta_{k3} + L_{1x}\tan\theta_{k1}\tan\theta_{k3} - L_{3x}}{\tan\theta_{k1}\tan\theta_{k3} - 1} \\ y_2 = \frac{(L_{3x} - L_{1x})\tan\theta_{k1} + L_{3y}\tan\theta_{k1}\tan\theta_{k3} - L_{1y}}{\tan\theta_{k1}\tan\theta_{k3} - 1} \end{cases} \quad (30)$$

or

$$\begin{cases} x_3 = \frac{(L_{3y} - L_{2y})\tan\theta_{k3} + L_{2x}\tan\theta_{k2}\tan\theta_{k3} + L_{3x}}{\tan\theta_{k2}\tan\theta_{k3} + 1} \\ y_3 = \frac{(L_{3x} - L_{2x})\tan\theta_{k2} + L_{3y}\tan\theta_{k2}\tan\theta_{k3} + L_{2y}}{\tan\theta_{k2}\tan\theta_{k3} + 1}. \end{cases} \quad (31)$$

Obviously, using only two of three collaborative BSs, the location of AV can be determined. For a better performance, the common strategy is to perform the average operation, and the resulting coordinates of $S(x, y)$ are given by

$$x = \frac{1}{3}\sum_{i=1}^{3} x_i, \quad y = \frac{1}{3}\sum_{i=1}^{3} y_i. \quad (32)$$

However, a direct application of the average operation may not always be a good choice for vehicle positioning, and the positioning accuracy may benefit from selecting a reliable subset of DOAs instead of the entire set [49], [50].

The received signal to noise ratios (SNRs) and the impinging DOAs of the same vehicle for different BSs could be quite different in practice. It is well known that if the received SNR of a BS is much lower than that of other BSs, and its corresponding DOA is close to the end of the visible region (i.e., $\theta \to \pm 90°$), then the DOA information provided by such a BS is no longer beneficial for the vehicle positioning and should be ignored.

Based on this observation, we propose to jointly exploit the received SNR and the impinging DOA information to select a more reliable subset/set of DOA estimates first, and then perform the AV positioning with preferred DOAs. Suppose that the received SNR of the ith BS to the kth source is pre-estimated in some way or simply estimated by

$$\text{SNR}_{i,k} = 10\lg\left(\hat{\mathbf{P}}_s(k,k)/\hat{\sigma}_n^2\right), i \in [1,3], k \in [1,K], \quad (33)$$
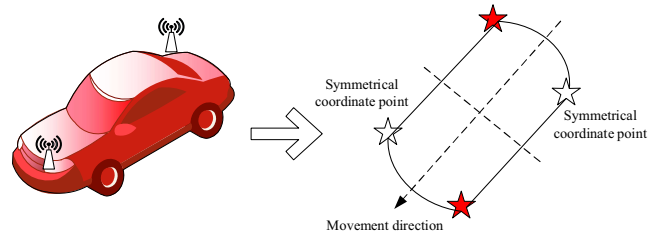

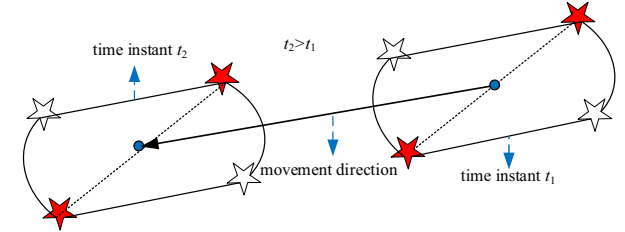Fig. 2. Scheme for contour extraction by installing two antennas.

Fig. 3. Illustration to obtain the information of vehicle movement direction.

where $\hat{\mathbf{P}}_s(k,k) = \hat{\mathbf{A}}^\dagger \hat{\mathbf{C}}^{-1}(\hat{\mathbf{R}}_r - \hat{\sigma}_n^2\mathbf{I}_M)(\hat{\mathbf{C}}^H)^{-1}(\hat{\mathbf{A}}^H)^\dagger$, and $\hat{\mathbf{A}}$ and $\hat{\mathbf{C}}$ are the estimates of $\mathbf{A}$ and $\mathbf{C}$ corresponding to the ith BS, respectively. In detailed implementation, when the difference between maximum SNR and minimum SNR is greater than 2 dB, the DOA corresponding to the minimum SNR will be ignored, and the reliable subset is built from the remaining two DOAs. On the other hand, if the received SNRs of three BSs are similar, we further select the reliable subset of DOAs according to the value of estimated DOAs. Specifically, if the absolute value of a DOA is greater than $75°$, it will be ignored, and the remaining two DOAs form the reliable subset. However, if the three DOAs can meet all the conditions above, they are supposed to be all reliable, and constitute the reliable set for positioning as a whole. The detailed procedure for selecting the reliable subset/set of DOA estimates for a certain AV positioning result is provided as **Algorithm 2**.

B. Vehicle Contour Extraction

Through extensive simulations, it is found that the proposed method is capable of achieving decimeter or even centimeter-level positioning accuracy for closely-spaced vehicles, which motivates us to further extract contour information of the vehicle by installing antennas with different identification labels on one vehicle. To achieve a reasonable contour extraction result, two key points need to be solved, i.e., configuration of suitable antennas and required DOA resolution capacity for the adopted DOA estimation method.

1) Configuration of antennas: In general, one can deploy multiple antennas on an AV with different carrier frequencies, which can provide an optimal and robust AV contour extraction result, since different wireless signals can be distinguished via bandpass filtering at the receiver side. However, such a deployment will undoubtedly increase system overhead and is also not in line with the current development trend of communication and sensing integration. Therefore, we here mainly consider the scenario that multiple antennas have
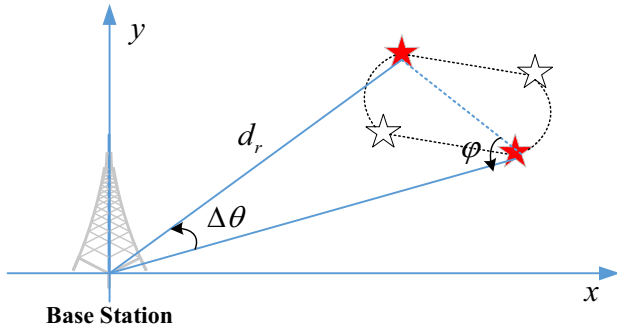
Fig. 4. Scene description for required DOA resolution capacity.

(a)

(b)

Fig. 5. RMSE and PO of DOA estimation versus SNR with $M = 50$, and $N = 100$, DOAs=$\{10°, 12°, 13°, 15°\}$.

the same carrier frequency. Under such a circumstance, installing two antennas with different identification labels on two diagonal positions of one vehicle will be a good choice, as depicted in Fig. 2. On the one hand, two antennas can effectively realize the extraction of AV contour information and simultaneously save the cost. On the other hand, more antennas with same frequency band are actually not conducive to effective antenna identification. To avoid ambiguity, the information of movement direction of the vehicle provided by the location information of two adjacent short period of time (i.e., $t_2 > t_1$ & $t_1 \rightarrow t_2$) is utilized here, whose principle is shown in Fig. 3. By combining the information of vehicle movement direction and the location of two antennas, the coarse contour of the vehicle can be determined.

2) Required DOA Resolution Capacity: High DOA resolution capacity of closely spaced antennas is a fundamental requirement for successful AV contour extraction. For simplicity, we only consider the required DOA resolution ability for one BS, the scene description and related parameter definitions are shown in Fig. 4. Suppose that the distance of two antennas for a given AV is fixed at d_f. Based on the trigonometric relationship, we have

$$\sin \Delta\theta = \frac{d_f}{d_r} \sin \varphi, \tag{34}$$

which implies that the required DOA resolution must satisfy

$$\Delta\theta \leq \arcsin \left[\frac{\sin \varphi}{d_r} d_f \right]. \tag{35}$$

Obviously, the resolution requirement increases as $\sin\varphi/d_r$ decreases. For instance, when $\varphi = 30°$, $d_f = 6$ m, and $d_r = 300$ m, $\Delta\theta \leq 0.573°$; while $\varphi = 40°$ and $d_r = 200$ m lead to $\Delta\theta \leq 1.105°$. Moreover, as φ may be a small value or even zero for certain orientation of the vehicle, the current BS cannot distinguish two antennas. Therefore, it is necessary to point out that the DOA resolution of at least two BSs must simultaneously satisfy (35) to ensure a continuity of contour extraction.

Remark 3: Note that the contour information of a vehicle is typically acquired by imaging methods [51], [52]. The proposed method provides another simple but effective way to extract the vehicle contour information, which is very useful and can be exploited as an auxiliary technology for safety driving in IoV environments.
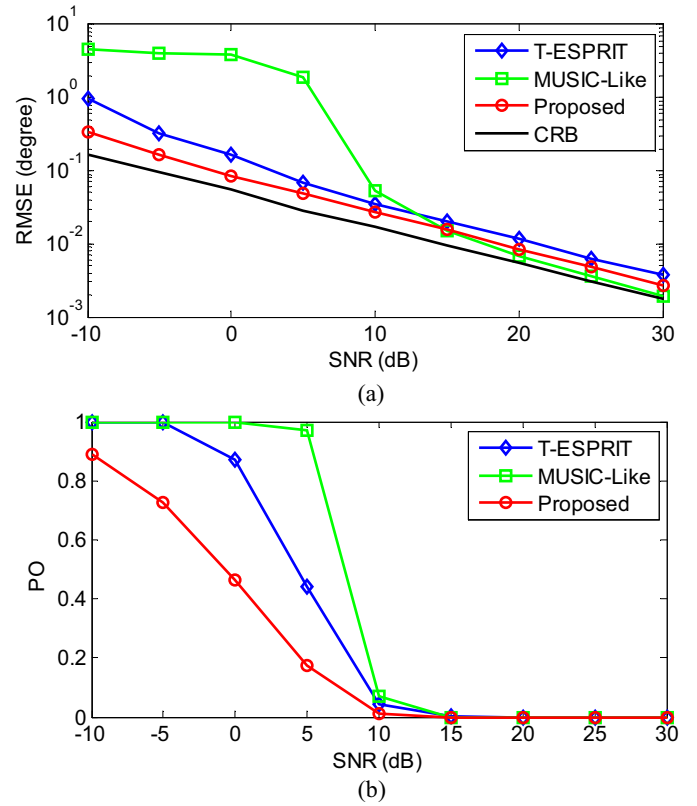
V. NUMERICAL SIMULATIONS

In this section, performance of the proposed method is evaluated in comparison with the traditional ESPRIT (using the mutual coupling elimination mechanism, and named as T-ESPRIT), the MUSIC-Like method in [33] and the CRB. The source signals are BPSK modulated with equal power, and the mutual coupling coefficients are set to be $\mathbf{c} = [1, 0.7e^{j\pi/5}, 0.3e^{-j\pi/12}]^T$. The inter-element distance d equals $\lambda/2$, and the SNR is defined as SNR $= 10 \log_{10}(\sigma_k^2/\sigma_n^2)$. Five metrics are adopted for performance evaluation. The first one is the root mean square error (RMSE) of DOA estimation. The second one is the probability of outlier (PO). The third one is the absolute error (AE) of AV positioning. The fourth one is the average runtime. And the last one is the AV contour extraction error (CEE). RMSE, PO, AE and CEE are respectively defined as

$$\text{RMSE} = \sqrt{\frac{1}{\bar{N}K} \sum_{\bar{n}=1}^{\bar{N}} \sum_{k=1}^{K} \Delta\bar{\theta}_{k,\bar{n}}^2}, \tag{36}$$

$$\text{PO} = 1 - \frac{1}{\bar{N}} \sum_{\bar{n}=1}^{\bar{N}} f\left(\Delta\theta_{k,\bar{n}}, 0.1°\right), \tag{37}$$

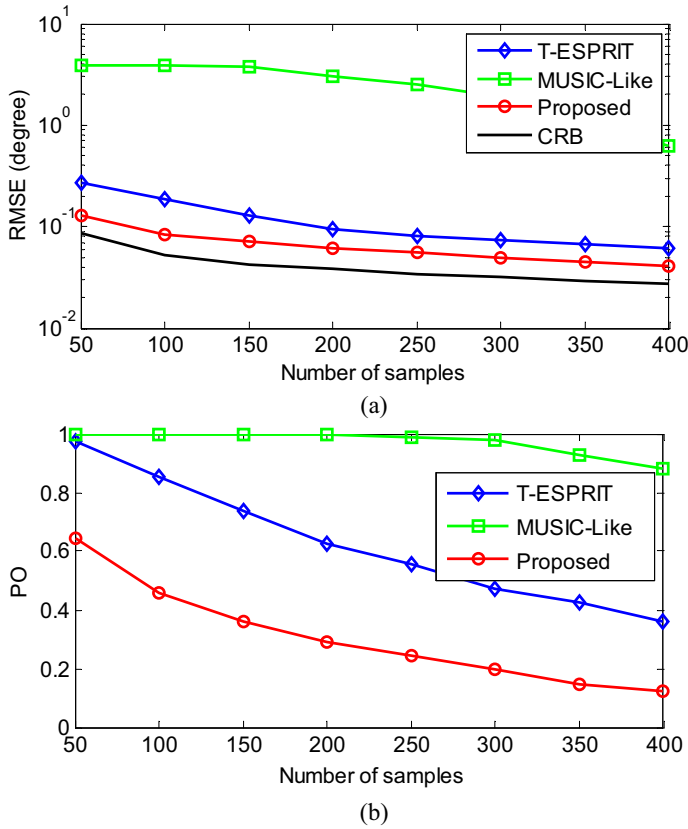$$\text{AE} = \frac{1}{K\bar{N}} \sum_{k=1}^{K} \sum_{\bar{n}=1}^{\bar{N}} d_{k,\bar{n}}, \tag{38}$$

Fig. 6. RMSE and PO of DOA estimation versus the number of samples N with SNR=0 dB, and $M = 50$, DOAs=$\{10°, 12°, 13°, 15°\}$.

Fig. 7. RMSE and PO of DOA estimation versus the number of sensors M with SNR=0 dB, and $N = 100$, DOAs=$\{10°, 12°, 13°, 15°\}$.

$$\text{CEE} = \frac{1}{\bar{N}} \sum_{\bar{n}=1}^{\bar{N}} (d_{1,\bar{n}} + d_{2,\bar{n}}), \tag{39}$$

where the parameter $\hat{\varsigma}_{k,\bar{n}}$ denotes the estimate of ς_k in the $\bar{n}$th Monte Carlo trial, $\Delta\theta_{k,\bar{n}} = |\hat{\theta}_{k,\bar{n}} - \theta_k|$, and $f(\Delta\theta_{k,\bar{n}}, 0.1°) = 1$ if and only if each $\Delta\theta_{k,\bar{n}} \leq 0.1°$, and $d_{k,\bar{n}}^2 = [(\hat{x}_{k,\bar{n}} - x_k)^2 + (\hat{y}_{k,\bar{n}} - y_k)^2]$. For all simulations below, $\bar{N}$ is fixed at 500.

A. DOA Estimation Performance Versus SNR

In the first simulation, we compare the DOA estimation performance for different methods at different SNRs, and their RMSE and PO curves are shown in Figs. 5(a) and 5(b), respectively. Four signals transmitted by four different AVs from DOAs $\{10°, 12°, 13°, 15°\}$ are considered. The number of searching grids in MUSIC-Like method is 1801 with a $0.1°$ interval. $M = 50$, $N = 100$, and SNR varies from -10 dB to 30 dB. It can be seen that the MUSIC-Like method suffers from a performance breakdown at 10 dB SNR, while the proposed one can avoid this effectively. As shown, our method outperforms the T-ESPRIT method in the whole SNR region and follows the CRB very well. Meanwhile, it also performs better than the MUSIC-Like method when SNR $\leq$ 15 dB; this robust performance plays an important role at the following stage for AV positioning. In addition, it should also be noted that the MUSIC-Like method outperforms the proposed one for SNR $>$ 15 dB, which can be explained as
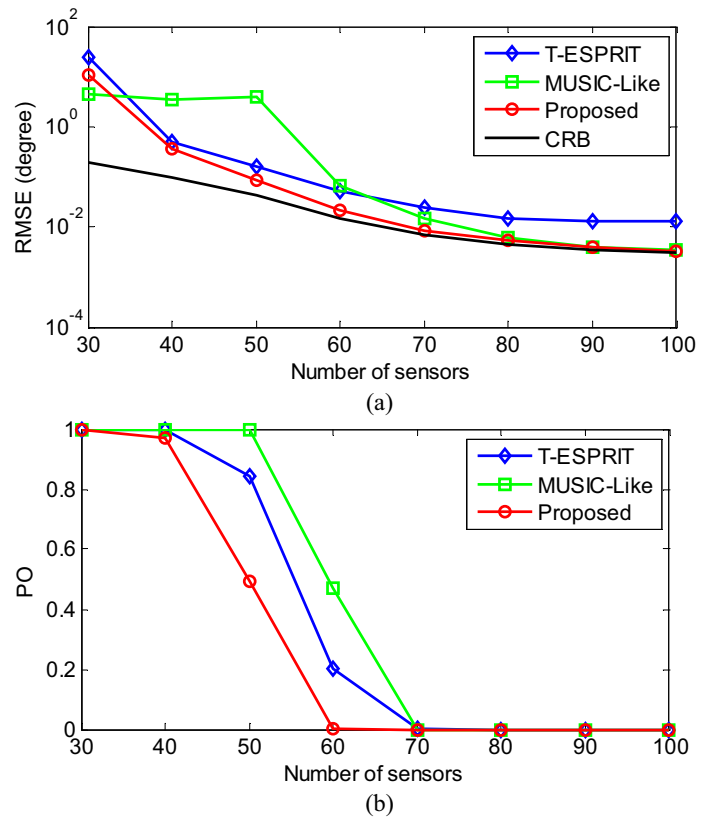
follows: there exists some array aperture loss for the proposed method in the presence of mutual coupling, and when the received SNR is large enough, the impact of array aperture loss on the DOA performance will be greater than that of the mutual coupling, leading to the under performance of the proposed method. Moreover, the PO indicates the resolution capability of the method to closely-spaced sources, as the minimum angle separation among four sources is only $1°$. Overall, we can say that the proposed method can achieve super resolution, and provides an effective way for high-performance AV positioning in actual IoV environments.

B. DOA Estimation Performance Versus N and M

In the second simulation, we examine the DOA estimation performance of the proposed method for different number of samples N and different number of sensors M. In Fig. 6, N varies from 50 to 400 in steps of 50 with SNR=0 dB, and $M = 50$, while in Fig. 7, M varies from 30 to 100 with SNR=0 dB, and $N = 100$. The other conditions are the same as in the first simulation. As can be seen from Figs. 6 and 7, the estimation performance of the proposed method becomes better with the increase of both N and M as expected. Meanwhile, the proposed method has again outperformed the other methods in terms of RMSE and PO. On the other hand, it can also be found that the performance of the MUSIC-Like method improves only slightly with the increase of N, as shown in Fig. 6, which can be explained in
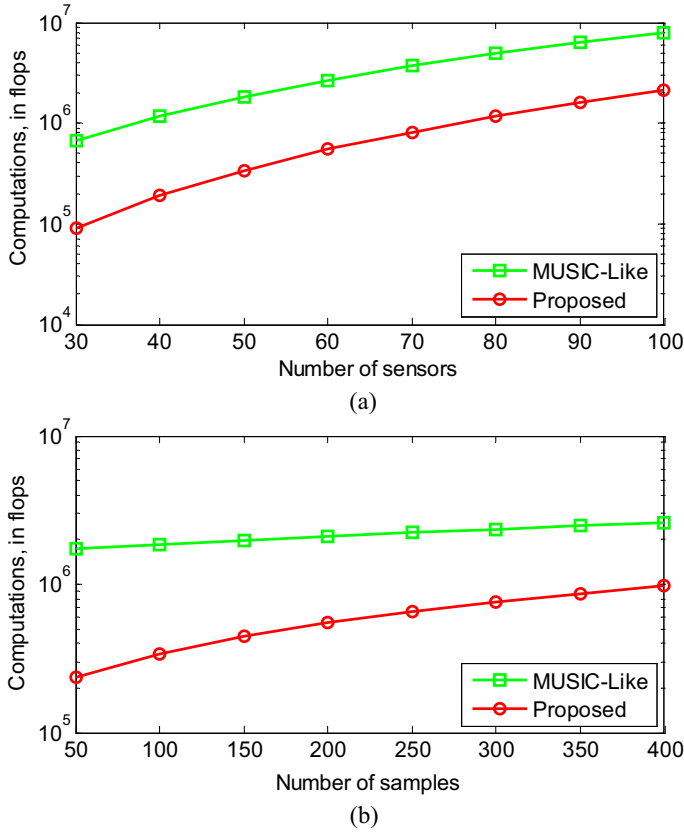
Fig. 8. Computational costs of the proposed method and the MUSIC-Like method versus M and N, with SNR=0 dB, DOAs=$\{10°, 12°, 13°, 15°\}$.
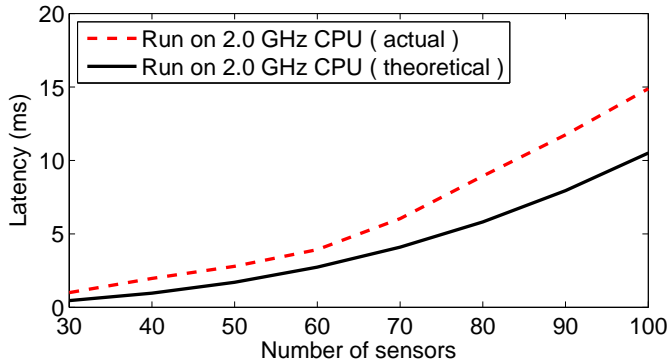
Fig. 9. Latency of positioning service versus M.

Fig. 10. AE of AV positioning versus SNR of BS1 with $M = 50$, $N = 100$. (a) *Scenario 1*. (b) *Scenario 2*.

Fig. 11. Availability with 0.3 m positioning accuracy versus M and SNR under the *Scenario 1* with $N = 100$.

that the four sources are not effectively distinguished for the MUSIC-Like method under the current simulation condition.

C. Average Runtime Versus M and N

Fig. 8 shows the computational cost required by the proposed method in comparison with the MUSIC-Like method for different M and N. The number of searching grids in MUSIC-Like method is 180 with a 1° interval. The other configurations are the same as those in Fig. 7. It can be clearly observed that the proposed method is computationally more efficient than the MUSIC-Like method, which implies that the proposed one is more suitable for real-time positioning requirement of AV. As
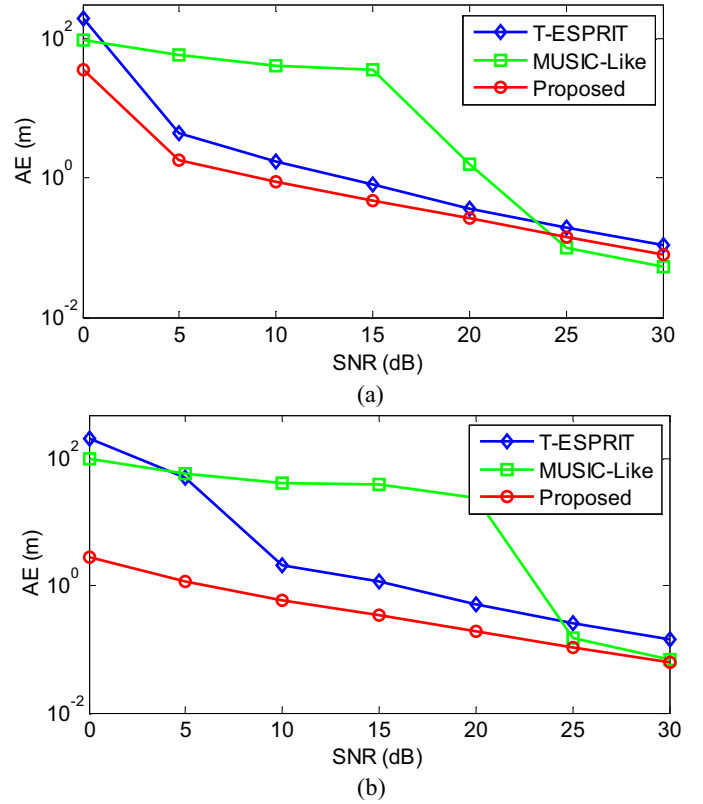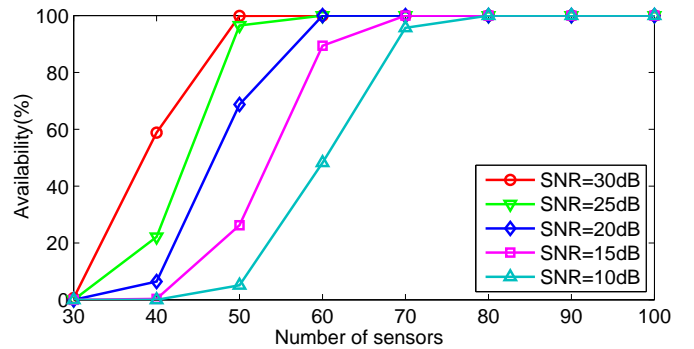
shown in Fig. 9, for $M \leq 80$ and $N = 100$, the proposed method can be carried out in less than nine milliseconds on MATLAB of a MacBook Pro laptop with Intel Core i5-2.0 GHz CPU and 3733 MHz LPDDR4X. That is, the proposed method can meet the 10 ms latency requirement of location services in 5G [38], [39]. Note that the actual latency is slightly larger than the theoretical one. This is because the CPU on the MacBook Pro laptop is also occupied by other applications.

D. AV Positioning Performance for Different SNRs

The AV localization performance of different methods is studied. The coordinates of three collaborative BSs are
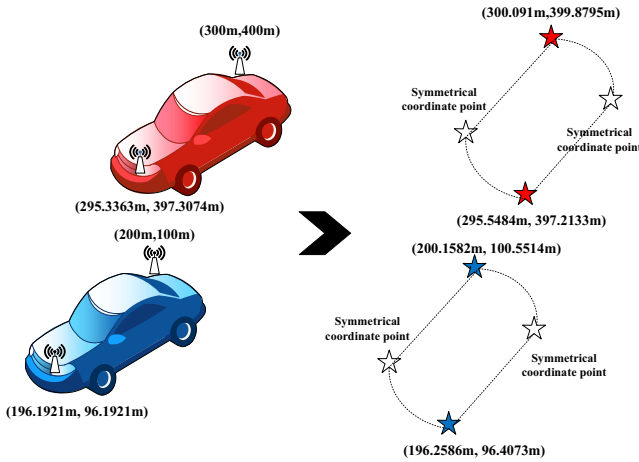
Fig. 12. Contour extraction result of the AV utilizing the proposed scheme, with $M = 50, N = 200$, and SNR=20 dB.

TABLE I
PROPOSED AV CONTOUR EXTRACTION RESULT

SNR(dB)	CEE (m)			
	N=200	N=300	N=400	N=500
0	4.9482	3.9208	3.7255	3.4132
5	2.8199	2.3376	2.0512	1.8086
10	1.6464	1.3051	1.0849	0.9530
15	0.8934	0.6965	0.6313	0.5497
20	0.5106	0.4195	0.3538	0.3194
25	0.2861	0.2223	0.2065	0.1783
30	0.1564	0.1229	0.1049	0.1010

$B_1(0 \text{ m}, 500 \text{ m})$, $B_2(0 \text{ m}, 0 \text{ m})$, and $B_3(600 \text{ m}, 0 \text{ m})$, respectively. The number of sensors M and the number of samples N at each BS are the same and equal to 50 and 100, respectively. Suppose that there are four AVs at the same plane with their locations being $S_1(395.4525 \text{ m}, 356.0671 \text{ m})$, $S_2(370.4931 \text{ m}, 357.7810 \text{ m})$, $S_3(395.7028 \text{ m}, 332.0341 \text{ m})$ and $S_4(85.5050 \text{ m}, 484.9232 \text{ m})$. Two different scenarios are considered. *Scenario 1*: the received SNR at each BS is the same. *Scenario 2*: the received SNRs of different BSs are different, and specifically, at BS3 it is 3 dB lower than those of BS1 and BS2. The simulation result with respect to *Scenario 1* is given in Fig. 10(a), from which we can see that the proposed method can achieve the submeter level accuracy when SNR$\geq$ 10 dB and the centimeter level when SNR$\geq$ 25 dB. This satisfactory performance demonstrates that it can provide a feasible way for the vehicle to realize autonomous and safe driving. The simulation result with respect to *Scenario 2* is given in Fig. 10(b), and it can be seen that when the received SNRs of different BSs are different, the localization performance of the compared methods based on the simple average operation degrades significantly. In comparison, the proposed one can provide a rather reliable performance under such a circumstance. Moreover, the availability result of the proposed method within 0.3 m positioning error is also tested under *Scenario 1*, as shown in Fig. 11, where $N = 100$ and M varies from 30 to 100. It can be seen that when SNR $\geq$ 10 dB and $M = 80$, the proposed method can yield a positioning accuracy within 0.3 m with 100% availability. Meanwhile, the running time of our method is less than 10 ms under these configurations, according to Fig. 9, which means that the proposed method can meet the requirements of an absolute position accuracy, the service availability and the latency for 5G localization, referring to the indicators corresponding to the 6th service level in 3GPP TS 22.261 [38], [39], which are 0.3 m, 99.9% and 10 ms, respectively.

E. Intuitive Result for Contour Extraction

Now, we provide an intuitive result for contour extraction of two AVs. The locations of antennas corresponding to two vehicles are shown in the left half of Fig. 12, and the extracted contour result is given in the right half of Fig. 12. The number of sensors M, the number of samples N and the received SNR at each BS are the same and equal to 50, 200 and 20 dB, respectively. By comparing the gap/difference between the true and estimated contours of two vehicles, we conclude that the proposed method is capable of accurate contour extraction of AVs. A more detailed design and realization on this aspect will be a topic of our future research.

F. Contour Extraction Performance versus SNR and N

In the last simulation, the AV contour extraction performance is further examined for different SNRs and number of samples N. The BS configuration is the same as in the fifth simulation, and an AV with coordinates of two antennas being $L_1(200\text{m}, 100\text{m})$ and $L_2(196.1921\text{m}, 96.1921\text{m})$ is considered. The number of sensors M is set to 100, while SNR and N vary from 0 dB to 30 dB in a step of 5 dB and 200 to 500 in a step of 100, respectively. The AV contour extraction result is shown in Table I. It can be seen that the proposed scheme can yield a good contour extraction performance, which in fact provides a feasible way for a safe and reliable autonomous driving.

VI. CONCLUSION

A novel method for AV positioning exploiting large-scale arrays has been proposed, where unknown mutual coupling is taken into account. Different from the state-of-the-art methods that utilize SCM and its corresponding eigenvectors directly, Toeplitz rectification and phase compensation are jointly applied to enhance the SCM and eigenvectors. As a result, the proposed method can provide a robust and super-resolution DOA estimation performance. Concerning the computational complexity, a shift invariance structure is constructed, which yields closed-form DOA solutions leading to the significant reduction in the computational complexity. Instead of using DOA estimates provided by multiple collaborative BSs directly, an effective approach has been developed to select a more reliable subset/set of DOA estimates first, and then achieve AV localization with preferred DOA information. Furthermore, given that the proposed method can reach the decimeter or even centimeter-level positioning accuracy, an antenna based scheme to extract the coarse contour information has been introduced, which is a good attempt from the DOA estimation perspective compared to the existing image based solutions.

REFERENCES

[1] A. Makkar and N. Kumar, "User behavior analysis-based smart energy management for webpage ranking: Learning automata-based solution," *Sustain. Computing: Informat. Syst.*, vol. 20, pp. 174-191, Dec. 2018.

[2] K. Jo, K. Chu, and M. Sunwoo, "Interacting multiple model filter-based sensor fusion of GPS with in-vehicle sensors for real-time vehicle positioning," *IEEE Trans. Intell. Transp. Syst.*, vol. 13, no. 1, pp. 329-343, Mar. 2012.

[3] Y. Song, Y. Fu, F. R. Yu, and L. Zhou, "Blockchain-enabled internet of vehicles with cooperative positioning: a deep neural network approach," *IEEE Internet of Things J.*, vol. 7, no. 4, pp. 3485-3498, Apr. 2020.

[4] S. Dwivedi *et al.*, "Positioning in 5G networks," *IEEE Communications Magazine.*, vol. 59, no. 11, pp. 38-44, Nov. 2021.

[5] H. Zhu, K. Yuen, L. Mihaylova, and H. Leung, "Overview of environment perception for intelligent vehicles," *IEEE Trans. Intell. Transp. Syst.*, vol. 18, no. 10, pp. 2584-2601, Oct. 2017.

[6] Y. Li, F. Shu, B. Shi, X. Cheng, Y. Song, and J. Wang, "Enhanced RSS-based UAV localization via tragectory and multi-base stations," *IEEE Commun. Lett.*, vol. 25, no. 6, pp. 1881-1885, Jun. 2021.

[7] G. Afifi and Y. Gadallah, "Autonomous 3-D UAV localization using cellular networks: deep supervised learning versus reinforcement learning approaches," *IEEE Access*, vol. 9, pp. 155234-155248, Nov. 2021.

[8] S. Saleh, A. S. EI-Wakeel, S. Sorour, and A. Noureldin, "Evaluation of 5G cell densification for autonomous vehicles positioning in urban settings," in *Proc. 2020 Int. Conf. Commun. Signal Process. and their Applications*, Sharjah, United Arab Emirates, Mar. 2021, pp. 1-6.

[9] Z.Z.M. Kassas, J. Khalife, K. Shamaei, and J. Morales, "I hear, therefore I know where I am: Compensating for GNSS limitations with cellular signals," *IEEE Signal Processing Mag.*, vo. 34, no.5, pp. 111-124, Sept. 2017.

[10] S. Saleh, S. Sorour, and A. Noureldin, "Vehicular positioning using mmWave TDOA with a dynamically tuned covariance matrix," in *Proc. IEEE Globecom Workshops*, Madrid, Spain, Dec. 2021, pp. 1-6.

[11] A. Saucan, T. Chonavel, C. Sintes, and J. Le Caillec, "CPHD-DOA tracking of multiple extended sonar targets in impulsive environments," *IEEE Trans. Signal Process.*, vol. 64, no. 5, pp. 1147-1160, Mar. 2016.

[12] A. Kangas and T. Wigren, "Angle of arrival localization in LTE using MIMO pre-coder index feedback," *IEEE Commun. Lett.*, vol. 17, no. 8, pp. 1584-1687, Aug. 2013.

[13] Z. M. Kassas and K. Shamaei, "A joint TOA and DOA acquisition and tracking approach for positioning with LTE signals," *IEEE Trans. Signal Process.*, vol. 69, 2689-2705, 2021.

[14] C. Xu, Z. Wang, Y. Wang, Z. Wang, and L. Yu, "Three passive TDOA-AOA receivers-based flying UAV positioning in extreme environment," *IEEE Sensors J.*, vol. 20, no. 16, pp. 9589-9595, Aug. 2020.

[15] R. O. Schmit, "Multiple emitter location and signal parameter estimation," *IEEE Trans. Antennas Propag.*, vol. 34, no. 3, pp. 276-280, Mar. 1986.

[16] R. Roy, A. Paulraj, and T. Kailath, "Estimation of signal parameters via rotational invariance techniques-esprit," in *Proc. IEEE 30th Annu. Tech. Symp. Ins. Soc. Optics Photon.*, Oct. 1986, vol.3, pp. 94-101.

[17] G. Liu, H. Chen, X. Sun, and R. C. Qiu, "Modified MUSIC algorithm for DOA estimation with nyström approximation," *IEEE Sensors J.*, vol. 16, no. 12, pp. 4673-4674, Jun. 2016.

[18] X. Yang, Y. Wang, and P. Chargé, "Modified DOA estimation with an unfolded co-prime linear array," *IEEE Commun. Lett.*, vol. 23, no. 5, pp. 859-862, May 2019.

[19] A. L. Kintz and I. J. Gupta, "A modified MUSIC algorithm for direction of arrival estimation in the presence of antenna array manifold mismatch," *IEEE Trans. Antennas Propag.*, vol. 64, no. 11, pp. 4836-4847, Nov. 2016.

[20] J. Lin, X. Ma, S. Yan, and C. Hao, "Time-frequency multi-invariance ESPRIT for DOA estimation," *IEEE Antennas Wireless Propag. Lett.*, vol. 15, pp. 770-773, 2016.

[21] A. Herzog and E. A. P. Habets, "Eigenbeam-ESPRIT for DOA-vector estimation," *IEEE Signal Process. Lett.*, vol. 26, no. 4, pp. 572-576, Apr. 2019.

[22] H. Chen, W. Wang, and W. Liu, "Augmented quaternion ESPRIT-type DOA estimation with a crossed-dipole array," *IEEE Commun. Lett.*, vol. 24, no. 3, pp. 548-552, Mar. 2020.

[23] X. Mestre and M. Á. Lagunas, "Modified subspace algorithms for DoA estimation with large arrays," *IEEE Trans. Signal Process.*, vol. 56, no. 2, pp. 598-614, Feb. 2008.

[24] P. Vallet, P. Loubaton, and X. Mestre, "Improved subspace estimation for multivariate observations of high dimension: the deterministic signals case," *IEEE Trans. Inf. Theory*, vol. 58, no. 2, pp. 1043-1068, Feb. 2012.

[25] P. Vallet and P. Loubaton, "Toeplitz rectification and DOA estimation with music," in *Proc. 2014 IEEE In. Conf. Acoust., Speech, Signal Process. (ICASSP)*, 2014, pp. 2237-2241.

[26] S. F. Cotter, "A two stage matching pursuit based algorithm for DOA estimation in fast time-varying environments," in *Proc. 2007 15th Int. Conf. Digital Signal Process.*, 2007, pp. 63-66.

[27] K. Aghababaiyan, V. Shah-Mansouri, and B. Maham, "High-precision OMP-based direction of arrival estimation scheme for hybrid non-uniform array," *IEEE Commun. Lett.*, vol. 24, no. 2, pp. 354-357, Feb. 2020.

[28] D. Malioutov, M. Cetin, and A. S. Willsky, "A sparse signal reconstruction perspective for source localization with sensor arrays," *IEEE Trans. Signal Process.*, vol. 53, no. 8, pp. 3010-3022, Aug. 2005.

[29] C. Zheng, G. Li, H. Zhang, and X. Wang, "An approach of DOA estimation using noise subspace weighted ℓ_1 minimization," in *Proc. IEEE In. Conf. Acoust., Speech, Signal Process. (ICASSP)*, 2011, pp. 2856-2859.

[30] X. Xu, X. Wei, and Z. Ye, "DOA estimation based on sparse signal recovery utilizing weighted l_1-norm penalty," *IEEE Signal Process. Lett.*, vol. 19, no. 3, pp. 155-158, Mar. 2012.

[31] J. Dai and H. C. So, "Sparse bayesian learning approach for outlier-resistant direction-of-arrival estimation," *IEEE Trans. Signal Process.*, vol. 66, no. 3, pp. 744-756, Feb. 2018.

[32] A. Das, "Real-valued sparse bayesian learning for off-grid direction-of-arrival (DOA) estimation in ocean acoustics," *IEEE J. Ocean. Eng.*, vol. 46, no. 1, pp. 172-182, Jan. 2021.

[33] F. Wen, J. Wang, J. Shi and G. Gui, "Auxiliary vehicle positioning based on robust DOA estimation with unknown mutual coupling," *IEEE Internet of Things J.*, vol. 7, no. 6, pp. 5521-5532, Jun. 2020.

[34] H. Wang, L. Wan, M. Dong, *et al.*, "Assistant vehicle localization based on three collaborative base stations via SBL-based robust DOA estimation," *IEEE Internet of Things J.*, vol. 6, no. 3, pp. 5766-5777, Jun. 2019.

[35] Y. Tian and H. Xu, "Calibration nested arrays for underdetermined DOA estimation using fourth-order cumulant," *IEEE Commun. Lett.*, vol. 24, no. 9, pp. 1949-1952, Sep. 2020.

[36] P. Chen, Z. Cao, Z. Chen, and X. Wang,"Off-grid DOA estimation using sparse bayesian learning in MIMO radar with unknown mutual coupling," *IEEE Trans. Signal Process.*, vol. 67, no. 1, pp. 208-220, Jan. 2019.

[37] K. Xiong, Z. Liu, and P. Wang, "SAGE-based algorithm for DOA estimation and array calibration in the presence of sensor location errors," *J. Syst. Eng. Electron.*, vol. 30, no. 6, pp. 1074-1080, Dec. 2019.

[38] A. Conti *et al.*, "Location awareness in beyond 5G networks," *IEEE Communications Magazine.*, vol. 59, no. 11, pp. 22-27, Nov. 2021.

[39] 3GPP Tech. Spec. Group Services and System Aspects, "Service requirements for the 5G system; Stage 1 (Release 18)," TS 22.261 V18.2.0 (2021-03), Mar. 2021.

[40] Y. Tian, Y. Qin, Z. Dong, and H. Xu, "DOA estimation of coherently distributed sources in massive MIMO systems with unknown mutual coupling," *Digital Signal Process.*, vol. 111, pp. 102987, Jan. 2021.

[41] H. Liu, L. Zhao, Y. Li, *et al.*, "A sparse-based approach for DOA estimation and array calibration in uniform linear array," *IEEE Sensors J.*, vol. 16, no. 15, pp. 6018-6027, Aug. 2016.

[42] J. Dai, X. Bao, N. Hu, C. Chang, and W. Xu, "A recursive RARE algorithm for DOA estimation with unknown mutual coupling," *IEEE Antennas Wireless Propag. Lett.*, vol. 13, pp. 1593-1596, 2014.

[43] P. Forster, "Generalized rectification of cross spectral matrices for arrays of arbitrary geometry," *IEEE Trans. Signal Process.*, vol. 49, no. 5, pp. 972-978, 2001.

[44] L. Huang and H. C. So, "Source enumeration via MDL criterion based on linear shrinkage estimation of noise subspace covariance matrix," *IEEE Trans. Signal Process.*, vol. 61, no. 19, pp. 4806-4821, Oct. 2013.

[45] L. Huang, Y. Xiao, K. Liu, *et al.*, "Bayesian information criterion for source enumeration in large-scale adaptive antenna array," *IEEE Trans. Veh. Technol.*, vol. 65, no. 5, pp. 3018-3032, May 2016.

[46] D. Paul, "Asymptotics of sample eigenstructure for a large dimensional spiked covariance model," *Statist. Sinica*, vol. 17, no. 4, pp. 1617-1642, 2017.

[47] B. Friedlander and A. J. Weiss, "Direction finding in the presence of mutual coupling," *IEEE Trans. Antennas Propag.*, vol. 39, no. 3, pp. 277-284, Mar. 1991.

[48] J. Xie, H. Tao, X. Rao, and J. Su, "Localization of mixed far-field and near-field sources under unknown mutual coupling," *Digital Signal Process.*, vol. 50, pp. 229-239, 2016.

[49] S. Joshi and S. Boyd, "Sensor selection via convex optimization," *IEEE Trans. Signal Process.*, vol. 57, no. 2, pp. 451-462, Feb. 2009.

[50] S. Bartoletti, A. Giorgetti, M. Z. Win and A. Conti, "Blind selection of representative observations for sensor radar networks," *IEEE Trans. Veh. Technol.*., vol. 64, no. 4, pp. 1388-1400, Apr. 2015.

[51] Z. Fan, J. Zhou, Da. Gao, and G. Rong, "Robust contour extraction for moving vehicle tracking," in *Proc. Int. Conf. Image Process.*, Rochester, NY, USA, 2002, pp. 625-628.

[52] P. Zhao, N. Wang, and Z. Pu, "Contour extraction of a moving vehicle in visible images based on image fusion," in *Proc. Int. Conf. Machine Learning and Cyber.*, Guangzhou, China, 2005, pp. 5216-5219.

Ye Tian (Member, IEEE) received the B.S. and Ph.D. degrees from the College of Communication Engineering, Jilin University, Changchun, China, in 2009 and 2014, respectively. He won a Huawei scholarship in 2013 and was selected as a young top talent by the Hebei Provincial Department of Education in 2016. He is currently an Associate Professor in Faculty of Electrical Engineering and Computer Science, Ningbo University. He has published more than 30 international peer-reviewed journal/conference papers and more than 10 patents. His research interests include array signal processing, autonomous vehicle positioning, massive MIMO as well as large-dimensional random matrix theory.

He Xu received the B.E. and M.E. degrees from the College of Communication Engineering, Jilin University, Changchun, China, in 2010 and 2013, respectively. From 2014 to 2020, she worked as a Research Assistant in Yanshan University. She is currently pursuing the Ph.D. degree in Faculty of Electrical Engineering and Computer Science, Ningbo University, Ningbo, China. Her main research interests include direction-of-arrival estimation, target positioning, integrated sensing and communication.

Wei Liu (Senior Member, IEEE) received the B.Sc. and L.L.B. degrees from Peking University, China, in 1996 and 1997, respectively, the M.Phil. degree from the University of Hong Kong in 2001, and the Ph.D. degree from the School of Electronics and Computer Science, University of Southampton, U.K., in 2003.

He then worked as a Postdoctoral Researcher first with Southampton and later with the Department of Electrical and Electronic Engineering, Imperial College London. Since September 2005, he has been with the Department of Electronic and Electrical Engineering, The University of Sheffield, U.K., first as a Lecturer and then a Senior Lecturer. He has published more than 300 journal and conference papers, five book chapters, and two research monographs titled *Wideband Beamforming: Concepts and Techniques* (John Wiley, March 2010) and *Low-Cost Smart Antennas* (Wiley-IEEE, March 2019), respectively. His research interests cover a wide range of topics in signal processing, with a focus on sensor array signal processing and its various applications, such as robotics and autonomous systems, human-computer interface, radar, sonar, satellite navigation, and wireless communications. He is a member of the Digital Signal Processing Technical Committee of the IEEE Circuits and Systems Society and the Sensor Array and Multichannel Signal Processing Technical Committee of the IEEE Signal Processing Society (Vice-Chair from January 2019). He was an Associate Editor of the IEEE TRANSACTIONS ON SIGNAL PROCESSING from March 2015 to March 2019. He is currently an Associate Editor of IEEE ACCESS, and an Editorial Board Member of the *Journal Frontiers of Information Technology and Electronic Engineering*.

Ming Jin (Member, IEEE) received the B.E. and Ph.D. degrees in electronic engineering from Xidian University, Xi'an, China, in 2005 and 2010, respectively. From 2013 to 2014, he was an Associate Researcher with the School of Electrical, Computer and Telecommunications Engineering, University of Wollongong, Wollongong, NSW, Australia. He is currently a Professor with the Faculty of Electrical Engineering and Computer Science, Ningbo University, Ningbo, China. His research interests include cognitive radio, optimization and machine learning.